



Thermophysical Evaluation of Silica Nanoparticles in Refrigerant Compressor Oil for Enhanced Refrigeration Performance

Adeel Ahmed Khan^{*}, Muhammad Ehtesham ul Haque^{*}

Department of Mechanical Engineering, NED University of Engineering and Technology, Karachi 75270, Pakistan

Corresponding Author Email: adeelahmedk@neduet.edu.pk

Copyright: ©2025 The authors. This article is published by IIETA and is licensed under the CC BY 4.0 license (<http://creativecommons.org/licenses/by/4.0/>).

<https://doi.org/10.18280/ijht.430118>

ABSTRACT

Received: 14 December 2024

Revised: 3 February 2025

Accepted: 18 February 2025

Available online: 28 February 2025

Keywords:

compressor, nanolubricant, thermal conductivity, viscosity

The thermo-physical properties of nanolubricants are essential for assessing their suitability in refrigeration systems. This study uses a two-step method to explore the preparation and characterization of a novel nanolubricant by dispersing SiO₂ nanoparticles into compressor lubricants. The composition of SiO₂ was analyzed via SEM-EDS and FTIR, while XRD confirmed its amorphous nature. Density, viscosity, and thermal conductivity were measured at room temperature for SiO₂ nanoparticles suspended in mineral and synthetic oils at different fractions (0.1%, 0.3%, 0.5%, and 0.7%) by volume. Performance improvements were compared to base lubricants. Results indicate that increasing SiO₂ concentration enhances density, viscosity, and thermal conductivity in both lubricant types. The highest density occurs at a 0.7% volume fraction, reaching 819.83 kg/m³ (mineral) and 861.22 kg/m³ (synthetic). The peak viscosity is also observed at 0.7%, measuring 36.97 mPa·s (mineral) and 65.39 mPa·s (synthetic). For synthetic nanolubricants, the maximum density increase (5.29%) appears at 0.3%, while viscosity rises by 77.81% at the same fraction. Thermal conductivity peaks at 0.7%, with values of 0.1105 W/m·K (mineral) and 0.1375 W/m·K (synthetic), achieving a 26.12% increase at 0.5%. The superior performance of synthetic nanolubricants over mineral ones suggests that they may enhance the efficiency of refrigeration systems.

1. INTRODUCTION

A substantial quantity of electricity is used by air conditioning and refrigeration equipment, making it critical to investigate energy-efficient refrigeration methods with eco-friendly refrigerants. An optimal refrigeration system should focus on maximizing efficiency. Enhancing the efficiency of a system is crucial for conserving energy and making it more energy-efficient. This helps to preserve existing energy resources and brings environmental aids, such as reduced greenhouse gas emissions and other contaminants. The main traditional methods for enhancing energy efficiency are improving insulation and upgrading to energy-efficient systems. Contrary to these conventional approaches, nanoparticles offer an innovative approach to improving system effectiveness [1-4].

Fluids with dispersed solid metallic particles are anticipated to have substantially greater thermal conductivities than ordinary heat transfer fluids. Introducing minute metallic or non-metallic particles, measured in nanometers, into conventional heat transfer fluids like water, ethylene glycol, and engine oil results in the formation of nanofluids [5]. A minute quantity of solid nanoparticles with greater thermal conductivity could be added to a base fluid to enhance heat transfer and improve thermophysical characteristics [6].

An alternative application for nanoparticles involves incorporating them into the lubricant employed in the

compressor [7]. The thermophysical properties of the selected base fluid can all be altered by nanoparticle addition, which improves compressor performance [8]. The prime role of oil is to improve compressor lubrication while also supplying cooling. Chemical stability, the lack of wax buildup, superior low-temperature performance, and compatibility with the compressor's parts are essential qualities of a successful lubricant [9]. The main drawback of conventional heat transfer fluids like ethanol, water, and heating oil is their low thermal conductivity. To improve heat transfer, high-conductivity particles at the millimeter or micrometer scale have been added to fluids [10].

The one-step method and the two-step method are the two methods used to create nanofluids. The first method involves the simultaneous production and scattering of nanoparticles within the fluid. This process eliminates the need for aeration, transportation, storage, and subsequent diffusion, resulting in a more uniform distribution and stable suspension of nanoparticles, which helps minimize agglomeration. The second approach uses chemical or physical techniques to create dry powders of nanoparticles, nanotubes, nanofibers, or nanomaterials. These particles are dispersed within a base fluid through magnetic force motion, ultrasonic stirring, high-shear blending, homogenization, or ball milling. While the one-step method offers better uniformity, it is more expensive and less suitable for large-scale production. On the other hand, the second approach is more economical for large-scale

production and has already been extensively utilized in industrial applications [11].

Numerous investigations have demonstrated that nanofluids contribute to the compressor's lower energy consumption. Akinlesi et al. [12] conducted an experiment using a 40 g charge of R-600a boosted with different concentrations of TiO₂ nano-lubricants (0 g/L and 0.2 g/L) in a domestic refrigerator utilizing R-12 and functioning under a specific ambient temperature environment. The findings show that, in comparison to the base fluid, energy consumption has decreased by 3.42 to 4.52%. Three different lubricants-SUNISO 3GS, POE oil, and SUNISO 3GS combined with nanoparticles- were compared in 2011, with R-134a as the refrigerant. When SUNISO 3GS was used instead of POE oil, an 18% drop in power consumption was observed. With the addition of nanoparticles, energy consumption decreased to 25% [13]. An experimental study used a nano-oil blend of polyalkylene glycol (PAG) enriched with Al₂O₃ nanoparticles in R-134a. A direct comparison between the performance of the PAG oil and the nano-oil mixture revealed notable results: the system's Coefficient of Performance (COP) surged by as much as 6.5%, along with the enhancement of condenser outlet sub-cooling [14].

An experiment was conducted by Jwo et al. [15] using R-134a as the primary refrigerant; incorporating 0.1% of Al₂O₃ nanoparticles by weight into refrigerant mineral oil (MO) raised the COP by 4.4%. It reduced the power utilization by 2.4%. An investigation contrasted R-600a and LPG refrigerants with TiO₂ nanolubricants. A nanolubricant was made by dissolving TiO₂ in MO at varying concentrations (0.2 g/l, 0.4 g/l, and 0.6 g/l). This setup utilized 1.94-33.33% less electricity for all R-600a refrigerant charges with 0.2 g/L of TiO₂ nano-lubricant than it did for baseline LPG refrigerant [16]. A study comparing the energy savings between using the HFC134a/nano-oil combination and HFC134a/polyester oil was conducted in 2008. Titanium oxide at 0.1% mass fraction was dispersed in MO to create nano-oil. The findings revealed a 26.1% decline in energy usage, and the increased oil return ratio clearly showed how nanoparticles boosted the solubility of MO and HFC134a [17].

A study by Husainy et al. [18] found that adding a 1% mass fraction of 50nm Copper Oxide nanoparticles to POE oil reduced compressor work by 21.37%. Combining TiO₂ nanolubricant with R134a refrigerant resulted in an 11% decrease in compressor work; however, utilizing SiO₂/PAG nanolubricant instead of TiO₂ with R134a increased COP by 24%. Vapor compression refrigeration systems (VCRS) overall performance was enhanced by introducing nano refrigerants and nanolubricants, which improved heat transmission, the refrigerant-oil combination, and tribological properties [19]. Researchers anticipate that the most efficient way to boost the efficacy of VCRS will be through nano refrigerants and nano lubricants. The COP rose by 21.42% in a test utilizing compressor oil made of PAG using R134a refrigerant and a 1.0% volume proportion of TiO₂ nanoparticles [20]. An experimental study was conducted using R-134a refrigerant in combination with SL-32 lubricant enhanced with Al₂O₃ nanolubricant. The comparison revealed a 0.913% reduction in current consumption and a 2.74% decrease in power when SL-32-Al₂O₃ nanolubricant was used instead of SL-32 lubricant under identical conditions at 31°C [21].

Senthilkumar et al. [22] experimented with hybrid nano-lubricants, incorporating two different nanoparticles, CuO and

SiO₂, at concentrations of 0.2 g/L and 0.4 g/L, respectively, in 40 g and 60 g of R-600a refrigerant. The findings demonstrated that the CuO and SiO₂ hybrid nano-lubricants led to an 18% upsurge in cooling capacity, a 35% enhancement in performance efficiency, and a drop of 75W in compressor power consumption. In another study, adding SiO₂ nano-oil to a compressor at mass fractions of 1%, 2%, and 2.5%, the setup COP enhanced by 7.61%, 14.05%, and 11.90%, respectively, compared to pure oil [23]. An experimental investigation evaluated the efficacy of a VCRS using an R-134a refrigerant with varying Al₂O₃ volume fractions (0.05%, 0.075%, 0.1%, and 0.2%) in MO. The results showed the highest COP enhancement of nearly 85% at a volume fraction of 0.075%. Additionally, when nanolubricant is utilized, the compressor's power consumption declines by approximately 27% compared to the base fluid [1].

An experimental investigation revealed that including nanoparticles led to a notable enhancement in cooling capability, especially when contrasted with the initial refrigeration-oil mixture's 70 W cooling capability. With the addition of TiO₂ nanoparticles, the cooling capacity rises to approximately 79 W, regardless of their concentration. Meanwhile, at 0.1 wt.% and 0.5 wt.%, adding Al₂O₃ nanoparticles raises the cooling capacity to 88 and 102 W, respectively [24]. For fluid simulations, a study used MWCNT/water nanofluid concentrations by volume (0.1%, 0.3%, and 0.5%); the gains in the heat transfer coefficient over water were 17%, 34%, and 47%, respectively [25].

This research uses a two-step approach to formulate a novel nanolubricant by integrating SiO₂ nanoparticles into compressor lubricants. This investigation contrasts synthetic lubricants with MO lubricants, both with and without incorporating SiO₂ nanoparticles. The materials used in the study and the process for creating the nanolubricant will be described in section 2, which also covers the experimental techniques. It will also outline the techniques used to measure density, assess viscosity, and calculate thermal conductivity. The results of several analytical methods used to examine the SiO₂ composition, such as SEM-EDS and FTIR analyses, will be presented in the results and discussion section of section 3, with XRD verifying the material's amorphous nature. The findings of density, viscosity, and thermal conductivity tests for SiO₂ nanoparticles distributed in mineral and synthetic oils at different volume fractions (0.1%, 0.3%, 0.5%, and 0.7%) carried out at room temperature will also be covered in detail in this section. The findings from the results and discussion section will be used to inform the conclusions in section 4.

According to the current literature, no prior studies specifically compare synthetic and mineral lubricants with SiO₂ at different volume fractions. These lubricants are already recognized for their efficacy, and the addition of nanoparticles seeks to evaluate the potential enhancements in characteristics such as density, viscosity, and thermal conductivity.

2. EXPERIMENTAL PROCEDURES

This section will outline the materials utilized in the research and the process for preparing the nanolubricant. This section also explains the procedure of density measurement, viscosity assessment, and the thermal conductivity calculation method used in this paper.

2.1 Materials

The SiO₂ nanoparticle used in this paper had a size of less than 100nm particle size procured from SIGMA ALDRICH USA, whose properties are listed in Table 1.

Table 1. Properties of nano particles [26]

Property	SiO ₂
Density (kg/m ³)	2400
Thermal conductivity, k (W/m·K)	1.4
Molecular mass, M (g/mol)	60.08
Average particle diameter, d _p (nm)	20
Specific heat, C _p (J/kg·K)	-36

Mineral and synthetic oils were used as lubricants in this study. Scanning electron microscopy (SEM) images were taken with a JEOL JAPAN JSM-IT 100 running at 20 kV with an associated energy dispersive spectroscopy (EDS) equipment to characterize and validate the purchased nanoparticles. A Panalytical X'pert Pro diffractometer was used for X-ray diffraction (XRD) to identify the product phase, and a Nicolet iS50 from Thermo Fisher Scientific, USA, was used for Fourier Transform Infrared Spectroscopy (FTIR) to analyze the crystal structure.

2.2 Preparation of nanofluid

Nanofluids are formed by combining metal or metallic oxide nanoparticles in base fluids like water, ethylene glycol, or oil. Adding nanoparticles modifies the thermophysical properties of the base fluid, improving compressor performance. At present, incorporating nanoparticles into lubricants or thermal fluids provides three main advantages: improving the refrigerant solubility in the lubricant, minimizing friction and wear through nanoparticle scattering, and enhancing lubricant thermal conductivity and heat transfer efficiency. These improvements in heat transfer from nanolubricants allow refrigeration systems to consume less electricity and use smaller compressors.

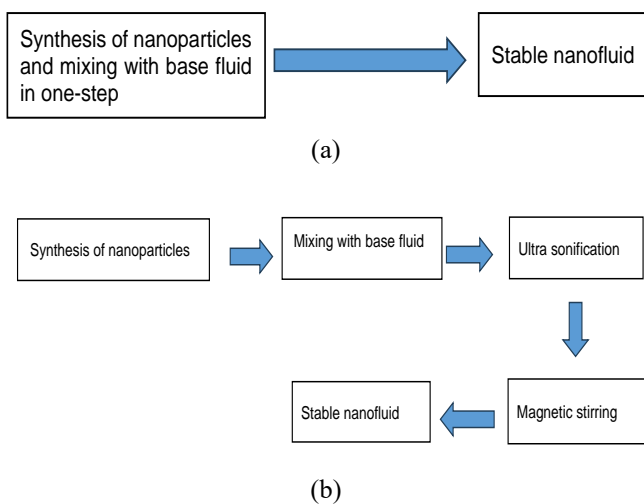


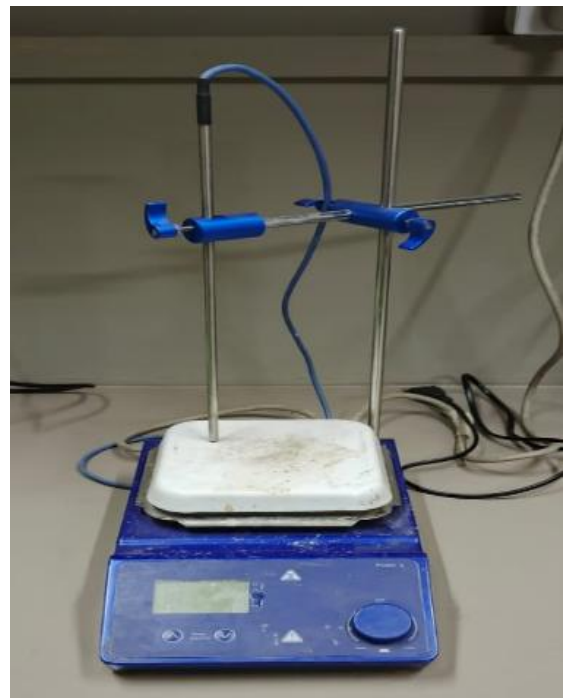
Figure 1. Nanofluid preparation methods: (a) one-step method and (b) two-step method

Preparing a stable nanolubricant involves blending a solid with a liquid. The one-step method simultaneously produces and disperses nanoparticles within the fluid (Figure 1(a)). In

this study, a two-step method (Figure 1(b)) was employed to formulate the nanolubricant; the same is utilized in the previous studies [27-30]. This process demands following specific guidelines, such as maintaining a stable and long-lasting suspension, preventing particle agglomeration, and avoiding any chemical changes to the fluid. In the initial stage, SiO₂ nanoparticles at different volume fractions were dispersed in MO, and their concentrations were determined using Eq. (1) [27]:

$$\varphi = \frac{m_p}{\rho_p} \div \left(\frac{m_p}{\rho_p} + \frac{m_f}{\rho_f} \right) \quad (1)$$

where, φ is the nanofluids volume fraction (%), m is the mass, and ρ is the density. The subscripts p and f denote particles and base fluid, respectively.



(a)



(b)

Figure 2. (a) Magnetic stirrer, (b) Ultrasonic bath

The mixture was stirred in the beaker using a magnetic stir bar, as shown in Figure 2(a). After that, the beaker was placed

on a hot plate stirrer, where the nanoparticle-lubricant mixture was heated and swirled at 70°C and 400 rpm for 30 minutes. Afterward, the nanolubricant was allowed to cool, transferred from the beaker to a glass bottle, and subjected to ultrasonication (Figure 2(b)) for 30 minutes to mix the lubricant and nanoparticles thoroughly. The mixture was subsequently observed for sedimentation to ensure stability, and throughout the 16-day [21] observation period, no significant settling was detected. This exact procedure was followed for the 0.3%, 0.5%, and 0.7% volume fractions in the MO. The same method is used to prepare SiO₂ nanolubricant with 0.1%, 0.3%, 0.5%, and 0.7% volume fractions in synthetic oil.

2.3 Measurement of density

The density is determined using a Relative Density (RD) bottle; the same is utilized by Sujith et al. [31]. First, the RD bottle is cleaned, dried, and weighed with a calibrated balance (Figure 3) to obtain the mass of the empty bottle (W_{RD}). Next, the bottle is filled with silica MO nanolubricant up to the designated mark, ensuring no air bubbles are present and that the combined weight of the bottle and nanolubricant is measured (W_{NL}). The mass of the silica MO nanofluid is calculated by subtracting the empty bottle's mass from the combined mass of the bottle and nanofluid ($W_{NL}-W_{RD}$). The volume is carved on the bottle. The density of the silica MO nanolubricant can be calculated using the formula [31].

$$\rho_{nl} = \frac{m_{nl}}{V} \quad (2)$$

where, ρ is the density, m is the mass, and V is the volume. The subscripts nl denote nanolubricant. A similar procedure is employed to find the density of the silica synthetic oil nanofluid.



Figure 3. Weighing balance

2.4 Measurement of viscosity

The kinematic viscosity of the nanofluids was assessed using a Poulten Selfe & Lee (PSL) Rheotek viscometer bath (Figure 4), adhering to the American Society for Testing and Materials (ASTM) D445 standard. Simultaneously, a Cannon-Fenske Opaque viscometer was immersed in the bath. This reverse-flow viscometer is specially engineered to measure kinematic viscosity by ASTM D445, making it well-suited for liquids where the meniscus is not visible at the timing marks, a limitation of the Cannon-Fenske Routine viscometer. It is also used to analyze lubricating oils at low temperatures and assess the impact of different additives on lubricating and hydraulic oils.

The Cannon-Fenske Opaque Reverse Flow Viscometer is specialized for measuring the viscosity of dark or opaque liquids where light does not pass easily. It permits the liquid to flow through a capillary tube from the upper reservoir toward the lower reservoir, with gravity providing the driving force. The liquid sample is placed in the upper reservoir, and the viscometer is placed in a temperature-controlled bath for precise viscosity measurement. As the liquid flows through the capillary tube, the time taken to pass two etched timing marks is recorded. The RHEOTEK ViscoCalc software, integrated with the bath, automates the determination of flow time and the calculation of kinematic viscosity. The PSL Rheotek software is pre-loaded with ASTM D445 result acceptance criteria and only reports results that meet these standards. All measurements are based on two consecutive flow times within the specified tolerance range.

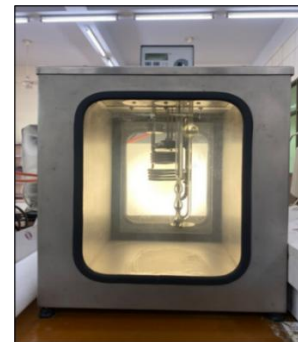


Figure 4. Viscometer in bath

2.5 Measurement of thermal conductivity

The thermal conductivity of liquids and gas equipment, illustrated in Figure 5, was utilized to determine the thermal conductivity of the nanofluid.

The setup includes two coaxial, concentric cylinder-shaped plugs with a small radial clearance of 0.3 mm to minimize natural heat convection. Heat is generated at the center of these copper plugs, which feature two ports for inserting and emitting the test fluid. The assembly is housed within a water jacket equipped with inlet and drain connections for temperature regulation. To monitor temperatures on the hot and cold surfaces of the test fluid, three thermocouples are placed on each of the heating and cooling cylindrical plugs. The inner plug has an outside diameter of 33.3 mm and a length of 100 mm, while the outside plug has an internal diameter of 33.9 mm. The stainless-steel water jacket cools the measuring cell and endures temperatures up to 150°C.



Figure 5. Thermal conductivity of liquid and gases

The system is linked to a control panel that provides power to the heater and digitally displays temperature readings. A potentiometer on the control panel allows the heating power to be adjusted. Thermal conductivity data were calibrated through tests using various fluids under different conditions to evaluate the effect of temperature differences on incidental heat transfer.

A cartridge heater, with a maximum power of 150 W and a high-temperature cut-off controller, generates heat flux in the sample gap. Type K thermocouples measure temperatures from 0 to 150°C, with six strategically placed in the inner and outer cylindrical plugs, cooling jackets, and heater surfaces to accurately capture temperature differences between the sample and external heat sources. The control panel features key components, such as a temperature controller with a thermocouple selector, a heater power regulator, digital displays for temperature and heater power, a main power switch, and a heater power switch. The cooling jacket of the outer coaxial cylinder is supplied by a constant source of clean, cool water at a stable temperature. An external thermostat, with a maximum capacity of 300°C, is connected to the cooling water inlet and outlet ports within a recirculation bath.

Fourier's Law is the cornerstone of conductive heat transfer, stating that heat flow (q) is directly proportionate to the temperature gradient (∂T) in a given direction (∂n). The thermal conductivity (k), a material property that varies with temperature, serves as the proportionality constant, while A represents the cross-sectional area perpendicular to the direction of heat movement.

$$q = -kA \frac{\partial T}{\partial n} \quad (3)$$

The test fluid is in a small annular area between two vertically orientated coaxial cylinders that make up the setup. An electrical heater is used to heat the inside cylinder. Fourier's Law, the governing equation, links the test fluid's thermal conductivity (k), internal cylinder temperature (T_1), external cylinder temperature (T_2), and heat output (Q).

$$k = \frac{\ln \frac{R_2}{R_1}}{(T_1 - T_2) * 2\pi * L} Q \quad (4)$$

where, R_1 and R_2 are the annulus radius filled with the liquid ($R_2 > R_1$), and L is the cylinder length.

After rearranging Eq. (3) to find k , we get:

$$k = \frac{q_c}{A} \frac{dx}{dT} \quad (5)$$

In the case of radial heat conduction within a cylinder, dx is replaced by dr , and the area A represents the cross-sectional area of the conductive channel. Under steady-state, the small radial gap, dr becomes Δr , and dT becomes ΔT , resulting in:

$$k = \frac{q_c}{A} \frac{\Delta r}{\Delta T} \quad (6)$$

By employing the conservation of energy equation in this system, the heat transfer by conduction (q_c) can be found:

$$q_c = q_{gen} - q_{lost} = q_{gen} - q_{lost} \quad (7)$$

The following expression for q_{lost} is obtained by combining Eq. (6) with Eq. (7):

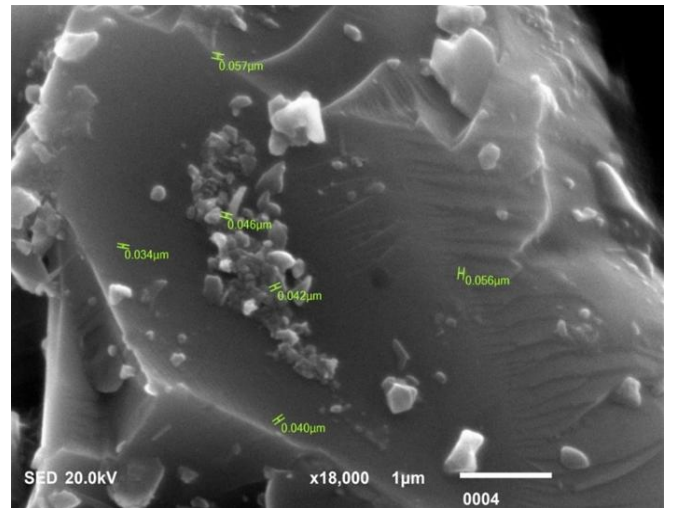
$$q_{lost} = q_{gen} - q_c = q_{gen} - kA \frac{\Delta T}{\Delta r} \quad (8)$$

$$q_{lost} = -kA \frac{\Delta T}{\Delta r} + q_{gen} - q_{con} - q_{rad} \quad (9)$$

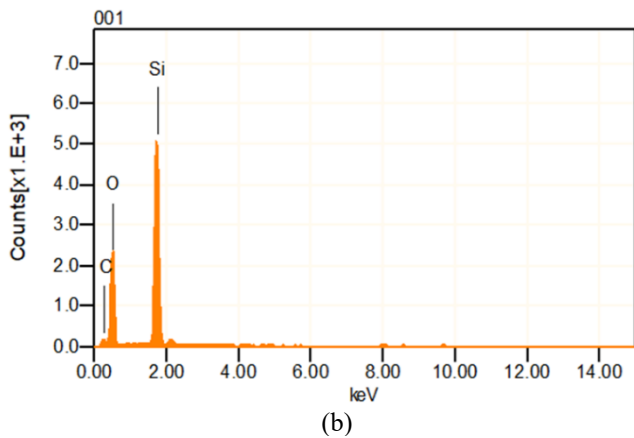
It is assumed that q_{lost} is proportionate to the temperature change between the plug and the jacket as described in Eq. (7), the heat generation for each point at specified conditions was held constant, and the losses occurred by the heat of convection and radiation was neglected. This assumption was assessed using linear regression analysis to calculate q_{lost} from the calibration graph, which plots incidental heat transfer against the temperature difference between the plug and the jacket. The thermal conductivity of a known standard solution, such as air (k_{air}), was used at each specified condition. The q_{lost} values obtained from the graph, and the calculated q_{gen} for fluid tests, were then substituted into Eq. (7). The experimental fluid thermal conductivity is subsequently determined with Eq. (4).

3. RESULTS AND DISCUSSIONS

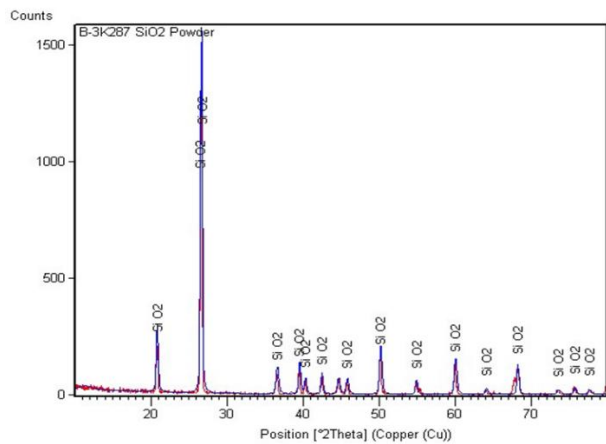
3.1 Scanning electron microscopy-Energy dispersive spectroscopy (SEM-EDS)



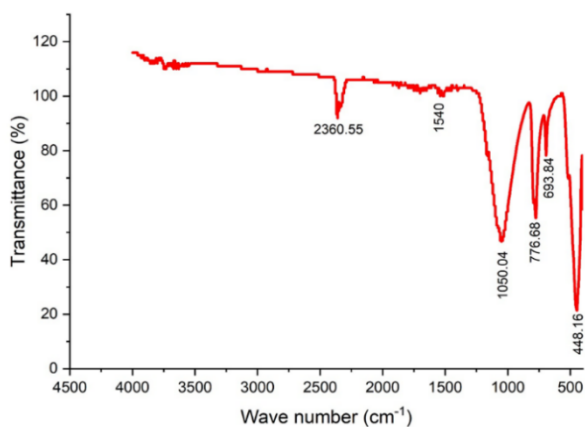
(a)



(b)



(c)



(d)

Figure 6. (a) SEM image of SiO₂ particles, (b) EDS of SiO₂ particles at 20KV showing silica predominate in the sample, (c) XRD of SiO₂ particles showing peaks, (d) FTIR of SiO₂ particles showing peaks

The nano size SiO₂ particles can be perceived in Figure 6(a). The SEM-EDS analysis of the sample, as portrayed in Figure 6(b), authorizes the purity of the silica product, with the dominant peaks corresponding to silicon and oxygen. Silicon and oxygen together make up 81.6% by atomic percentage, while the remaining 18.4% is attributed to minor peaks from carbon.

3.2 X-Ray diffraction (XRD)

As illustrated in Figure 6(c), the diffraction patterns were

obtained using Cu-K α radiation ($\lambda=1.5418 \text{ \AA}$) with an operating voltage of 40kV and a current of 30 mA. The XRD pattern of the samples was recorded in the 2θ range from 10° to 80° , with a step size of 0.025° . A broad, amorphous peak was observed, corresponding to a Bragg angle of $2\theta=26.7092^\circ$. The same results are also highlighted by the Standard X-ray diffraction Powder Patterns National Bureau of Standards (NBS) monograph U.S. Department of Commerce [32].

3.3 Fourier transform spectroscopy (FTIR)

The FTIR test was conducted using a Nicolet iS50 Thermo Fisher Scientific USA, with samples scanned over a range of 400 to 4,000 cm^{-1} at a resolution of 0.48 cm^{-1} . The FT-IR spectrum of the silica Figure 6(d) reveals characteristic functional groups associated with pure silicon dioxide at 1050.04, 777, 694, and 449 cm^{-1} .

The prominent and wide IR band at 1050.04 cm^{-1} is typically attributed to the transversal optical (TO) and longitudinal optical (LO) modes of the Si-O-Si asymmetric stretching vibrations. The vibration peaks corresponding to the SiO₂ groups are assigned to the asymmetric and symmetric stretching modes (observed at 1050.04 and 777 cm^{-1}) and the bending mode (449 cm^{-1}), the latter appearing as a weak band. The sharp peak observed at 826 cm^{-1} is associated with Si-O-Si symmetric stretching vibrations, while the IR band at 449 cm^{-1} corresponds to Si-O-Si bending vibrations. These findings confirm the successful condensation reaction between Si-OR groups [33].

3.4 Density

As revealed in Figure 7 for 0.1%, 0.3%, 0.5%, and 0.7% particle loadings, the density rise in silica MO nanolubricant density as compared to MO lubricant is 0.71%, 1.08%, 1.53%, and 1.98% respectively. The improvement in the density of silica nanoparticles with synthetic lubricant as compared to synthetic lubricant for 0.1%, 0.3%, 0.5%, and 0.7% volume fraction is 0.83%, 1.34%, 1.73%, and 2%, respectively. When comparing the density growth in synthetic nanolubricant as compared to mineral nanolubricant for 0.1%, 0.3%, 0.5%, and 0.7% volume fraction, the upsurge is 5.15%, 5.29%, 5.23%, and 5.05% respectively. The highest density value is calculated at a 0.7% volume fraction for mineral and synthetic lubricants, measuring 819.83 kg/m^3 and 861.22 kg/m^3 , respectively.

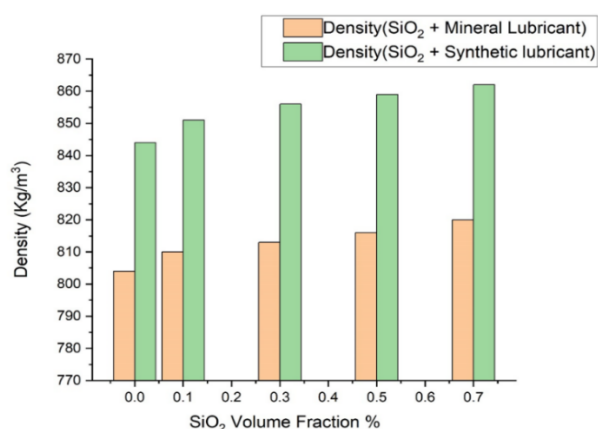


Figure 7. Density comparison of silica nano particles with mineral oil and silica nano particles with synthetic lubricant

Solid-liquid suspensions have a greater density than base fluids because solid particles are much denser than the molecules of liquids and gases [34].

3.5 Viscosity

The bar graphs in Figure 8 show that for 0.1%, 0.3%, 0.5%, and 0.7% particle loadings, the increment in viscosity of silica MO nano lubricant as compared to MO lubricant is 5.84%, 6.74%, 8.01%, and 9.29% respectively. The enhancement in viscosity of silica nanoparticles with synthetic lubricant compared to synthetic lubricant for 0.1%, 0.3%, 0.5%, and 0.7% volume fraction is 1.3%, 2.51%, 3.53%, and 4.43%, respectively. When comparing the viscosity growth in synthetic nanolubricant as compared to mineral nanolubricant for 0.1%, 0.3%, 0.5%, and 0.7% volume fraction, the upsurge is 77.2%, 77.81%, 77.46%, and 76.9% respectively. The maximum viscosity is recorded at a 0.7% volume fraction for mineral and synthetic lubricants, with 36.97 mPa-s and 65.39 mPa-s values, respectively.

The nanofluids viscosity rises in tandem with the nanoparticle's concentrations by volume. This is because nanoparticles' more significant surface area than the surrounding fluid leads to more particle collisions and interactions. These interactions can increase viscosity by impeding fluid flow and strengthening its resistance to shearing or deformation. The nanoparticles increase friction by acting as barriers in the fluid, making it harder to flow freely [35].

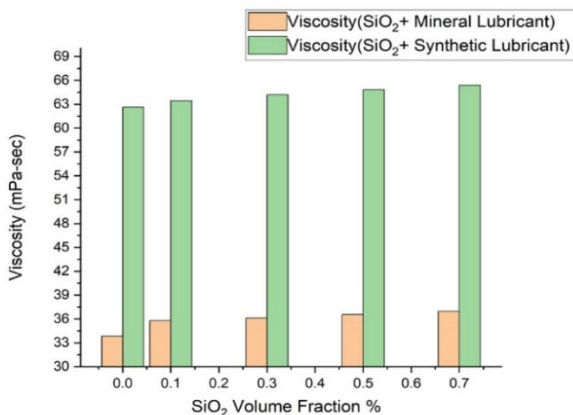


Figure 8. Viscosity comparison of silica nano particles with mineral oil and silica nano particles with synthetic lubricant

3.6 Thermal conductivity

As shown in Figure 9, for silica nanoparticle volume fractions (0.1%, 0.3%, 0.5%, and 0.7%), the thermal conductivity of silica MO nanolubricants increased by 1.99%, 4.02%, 5.38%, and 18.23%, respectively, compared to MO lubricant. For silica nanoparticles in synthetic lubricants, the thermal conductivity increases by 4.64%, 11.56%, 21.70%, and 34.77%, respectively, compared to synthetic lubricants. When comparing the thermal conductivity increase in synthetic nanolubricants to mineral nanolubricants, the gains are 12.06%, 17.13%, 26.12%, and 24.49%, respectively, for the same volume fractions. The maximum thermal conductivity is calculated at a 0.7% volume fraction for mineral and synthetic lubricants, with values of 0.1105 W/m·K and 0.1375 W/m·K, respectively.

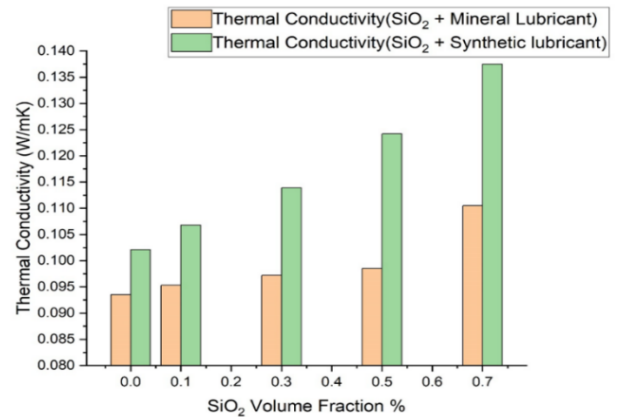


Figure 9. Thermal conductivity comparison of silica nano particles with mineral oil and silica nano particles with synthetic lubricant

The inclusion of nanoparticles improved the base oil's thermal conductivity, and the nanofluid's average thermal conductivity increased as the nanoparticles' volume concentration increased. This could be due to the nanoparticles spread within the base oil, which help foster the formation of a micro-convection effect [36] and the formation of base oil layers on solid nanoparticle surfaces [37]. The number of collisions is increased when the base lubricant contains nanoparticles. Furthermore, it increases the surface-to-volume ratio, which enhances thermal conductivity [16, 38].

4. CONCLUSION

This study determined the thermo-physical characteristics of SiO₂ nanoparticles in mineral and synthetic lubricants at volume fractions of 0.1%, 0.3%, 0.5%, and 0.7% at room temperature. The significant findings are as follows.

(a) The density of both mineral and synthetic lubricants rises with a higher nanoparticle volume fraction. Specifically, the silica MO nanolubricant exhibits a maximum density increase of 1.98% at a 0.7% volume fraction compared to MO lubricant. Similarly, the density of silica nanoparticles in synthetic lubricant shows the highest increase of 2% at the same volume fraction. Furthermore, when comparing the density growth between synthetic and mineral nanolubricants, the most significant rise is 5.29% at a 0.3% volume fraction.

(b) The viscosity of the nanolubricant rises with higher nanoparticle concentrations, though the extent of this increase differs between the two types of nanolubricants at the same volume fraction. The silica MO nanolubricant exhibits a maximum viscosity increase of 9.29% compared to the base MO lubricant at a 0.7% volume fraction. Similarly, the highest viscosity enhancement for silica nanoparticles in synthetic lubricant is 4.23% at the same volume fraction. When comparing viscosity variations between synthetic and mineral nanolubricants, the most significant increase is 77.81%, observed at a 0.3% volume fraction.

(c) The thermal conductivity of the nanolubricant increases with higher nanoparticle concentrations; however, the extent of the increase differs between the two types of nanolubricants at the same volume fraction. The silica MO nanolubricant shows a maximum thermal conductivity enhancement of 18.23% over the base MO lubricant at a 0.7% volume fraction. In comparison, the highest thermal conductivity increase for

silica nanoparticles in synthetic lubricant is 34.77% at the same volume fraction. When comparing the thermal conductivity enhancement in synthetic nanolubricants to mineral nanolubricants, the most significant rise is 26.12%, observed at a 0.5% volume fraction.

The findings suggest that incorporating nanoparticles into compressor lubricants enhances their thermophysical properties, potentially enhancing refrigeration systems' performance. The silica nanolubricants in this study were specifically designed for testing in residential refrigerant compressors. To advance this research, further investigation is required to evaluate the efficacy of SiO₂ nanoparticle-based compressor lubricants across varying temperatures.

ACKNOWLEDGMENT

This work is supported by the Ministry of Science and Technology (MoST) Endowment Fund vide office order No. Acad/50(48)/597 dated 02nd January 2024.

REFERENCES

- [1] Subhedar, D.G., Patel, J.Z., Ramani, B.M. (2022). Experimental studies on vapour compression refrigeration system using Al₂O₃/mineral oil nanolubricant. *Australian Journal of Mechanical Engineering*, 20(4): 1136-1141. <https://doi.org/10.1080/14484846.2020.1784558>
- [2] Hussein, A.T., Abedalh, A.S., Alomar, O.R. (2023). Enhancement performance of vapor compression system using nano copper oxide lubricant inside compressor and a fluidized bed for condenser cooling. *Case Studies in Thermal Engineering*, 44: 102819. <https://doi.org/10.1016/j.csite.2023.102819>
- [3] Azman, N.F., Samion, S., Paiman, Z., Hamid, M.K.A. (2024). Tribological performance and mechanism of graphite, hBN and MoS₂ as nano-additives in palm kernel oil-Based lubricants: A comparative study. *Journal of Molecular Liquids*, 410: 125616. <https://doi.org/10.1016/j.molliq.2024.125616>
- [4] Mohammed, K.H., Al-Mirani, A.E., Ali, B.M., Alomar, O.R. (2024). Impacts of using Al₂O₃ nano particle to compressor oil on performance of automobile air conditioning system. *Frontiers in Heat and Mass Transfer*, 22(3): 839-854. <https://doi.org/10.32604/fhmt.2024.052671>
- [5] Choi, S.U., Eastman, J.A. (1995). Enhancing thermal conductivity of fluids with nanoparticles (No. ANL/MSD/CP-84938; CONF-951135-29). Argonne National Lab.(ANL), Argonne, IL (United States).
- [6] Ma, T., Guo, Z., Lin, M., Wang, Q. (2021). Recent trends on nanofluid heat transfer machine learning research applied to renewable energy. *Renewable and Sustainable Energy Reviews*, 138: 110494. <https://doi.org/10.1016/j.rser.2020.110494>
- [7] Majgaonkar, A. (2016). Use of nanoparticles in refrigeration systems: A literature review paper. In *International Refrigeration and Air Conditioning Conference*.
- [8] Hatami, M., Jing, D. (2020). *Nanofluids: Mathematical, Numerical, and Experimental Analysis*. Elsevier.
- [9] Hundy, G.H., Trott, A.R., Welch, T.C. (2008). Oil in refrigerant circuits. *Refrigeration and Air-Conditioning: Butterworth-Heinemann*, 89-98. <https://www.sciencedirect.com/book/9780081006474/refrigeration-air-conditioning-and-heat-pumps>.
- [10] Guo, Z. (2020). A review on heat transfer enhancement with nanofluids. *Journal of Enhanced Heat Transfer*, 27(1): 1-70. <https://doi.org/10.1615/JEnhHeatTransf.2019031575>
- [11] Yu, W., Xie, H. (2012). A review on nanofluids: Preparation, stability mechanisms, and applications. *Journal of Nanomaterials*, 2012(1): 435873. <https://doi.org/10.1155/2012/435873>
- [12] Akinlesi, L.J., Adelekan, D.S., Ohunakin, O.S., Atiba, O.E., Gill, J., Atayero, A.A. (2019). Experimental performance of a domestic refrigerator with TiO₂-nanoparticles operating within selected ambient temperature. *Journal of Physics: Conference Series. IOP Publishing*, 1378(4): 042081. <http://doi.org/10.1088/1742-6596/1378/4/042081>
- [13] Subramani, N., Prakash, M.J. (2011). Experimental studies on a vapour compression system using nanorefrigerants. *International Journal of Engineering, Science and Technology*, 3(9): 95-102. <http://doi.org/10.4314/ijest.v3i9.8>
- [14] Nair, V., Parekh, A.D., Tailor, P.R. (2020). Experimental investigation of a vapour compression refrigeration system using R134a/Nano-oil mixture. *International Journal of Refrigeration*, 112: 21-36. <https://doi.org/10.1016/j.ijrefrig.2019.12.009>
- [15] Jwo, C.S., Jeng, L.Y., Teng, T.P., Chang, H. (2009). Effects of nanolubricant on performance of hydrocarbon refrigerant system. *Journal of Vacuum Science & Technology B: Microelectronics and Nanometer Structures Processing, Measurement, and Phenomena*, 27(3): 1473-1477. <https://doi.org/10.1116/1.3089373>
- [16] Jatinder, G., Ohunakin, O.S., Adelekan, D.S., Atiba, O.E., Daniel, A.B., Singh, J., Atayero, A.A. (2019). Performance of a domestic refrigerator using selected hydrocarbon working fluids and TiO₂-MO nanolubricant. *Applied Thermal Engineering*, 160: 114004. <https://doi.org/10.1016/j.applthermaleng.2019.114004>
- [17] Bi, S.S., Shi, L., Zhang, L.L. (2008). Application of nanoparticles in domestic refrigerators. *Applied Thermal Engineering*, 28(14-15): 1834-1843. <https://doi.org/10.1016/j.applthermaleng.2007.11.018>
- [18] Husainy, A.S., Chougule, P., Hasure, S., Patil, A., Tukshetti, S., Badade, K. (2019). Performance improvement of ducted air-conditioning system with different mass fraction of CuO nanoparticles mixed in POE oil. *International Research Journal of Engineering and Technology (IRJET)*, 6(4): 1003-1007.
- [19] Sharif, M.Z., Azmi, W.H., Mamat, R., Shaiful, A.I.M. (2018). Mechanism for improvement in refrigeration system performance by using nanorefrigerants and nanolubricants-A review. *International Communications in Heat and Mass Transfer*, 92: 56-63. <https://doi.org/10.1016/j.icheatmasstransfer.2018.02.012>
- [20] Selimefendigil, F. (2019). Experimental investigation of nano compressor oil effect on the cooling performance of a vapor-Compression refrigeration system. *Journal of Thermal Engineering*, 5(1): 100-104. <https://doi.org/10.18186/thermal.513023>
- [21] Khan, A.A., ul Haque, M.E., Siddiqui, F., Nasir, S.M.T.,

- Shafique, T., Khalid, H. (2024). Reducing energy consumption of refrigerator compressor using aluminum oxide nanoparticles. *Memoria Investigaciones en Ingeniería*, (26): 38-53. <https://doi.org/10.36561/ING.26.3>
- [22] Senthilkumar, A., Abhishek, P.V., Adithyan, M., Arjun, A. (2021). Experimental investigation of CuO/SiO₂ hybrid nano-Lubricant in R600a vapour compression refrigeration system. *Materials Today: Proceedings*, 45: 6083-6086. <https://doi.org/10.1016/j.matpr.2020.10.178>
- [23] Desai, N.S., Patil, P.R. (2015). Application of SiO₂ nanoparticles as lubricant additive in VCRS: An experimental investigation. *Asian Review of Mechanical Engineering*, 4(1): 1-6. <https://doi.org/10.51983/arme-2015.4.1.2393>
- [24] Yousif, S.S., Al-Obaidi, M.A., Al-Muhsen, N.F. (2024). Towards more efficient refrigeration: A study on the use of TiO₂ and Al₂O₃ nanoparticles. *International Journal of Heat & Technology*, 42(4): 1251-1256, <https://doi.org/10.18280/ijht.420415>
- [25] Nadhim, A.A., Alderoubi, N., Al-Tameri, O.H.A., Mustafa, M.A.S., Majdi, H.S. (2024). Numerical study of heat transfer in helical cone coil heat exchanger using MWCNT-Water Nanofluid. *International Journal of Heat & Technology*, 42(5). <https://doi.org/10.18280/ijht.420510>
- [26] Aldrich, S. Silica dioxide nano particles. <https://www.sigmaaldrich.com/PK/en/product/aldrich/637246>, accessed on Nov.19, 2024.
- [27] Ismail, M.F., Azmi, W.H., Mamat, R., Ab Rahim, R. (2022). Rheological behaviour and thermal conductivity of polyvinyl ether lubricant modified with SiO₂-TiO₂ nanoparticles for refrigeration system. *International Journal of Refrigeration*, 138: 118-132. <https://doi.org/10.1016/j.ijrefrig.2022.03.026>
- [28] Zawawi, N.N.M., Azmi, W.H., Redhwan, A.A.M., Sharif, M.Z., Sharma, K.V. (2017). Thermo-physical properties of Al₂O₃-SiO₂/PAG composite nanolubricant for refrigeration system. *International Journal of Refrigeration*, 80: 1-10. <https://doi.org/10.1016/j.ijrefrig.2017.04.024>
- [29] Qing, S.H., Rashmi, W., Khalid, M., Gupta, T.C.S.M., Nabipoor, M., Hajibeigy, M.T. (2017). Thermal conductivity and electrical properties of hybrid SiO₂-graphene naphthenic mineral oil nanofluid as potential transformer oil. *Materials Research Express*, 4(1): 015504. <https://doi.org/10.1088/2053-1591/aa550e>
- [30] Sidik, N.A.C., Jamil, M.M., Japar, W.M.A.A., Adamu, I.M. (2017). A review on preparation methods, stability and applications of hybrid nanofluids. *Renewable and Sustainable Energy Reviews*, 80: 1112-1122. <https://doi.org/10.1016/j.rser.2017.05.221>
- [31] Sujith, S.V., Solanki, A.K., Mulik, R.S. (2021). Experimental investigations on viscosity and density of eco-Friendly MoS₂-Sesame oil nano-Lubricants and its influence on pumping power. *Nanotechnology*, 32(36): 365702. <http://doi.org/10.1088/1361-6528/ac074c>
- [32] Morris, M.C. (1981). Standard x-ray diffraction powder patterns: section 18- data for 58 substances. NBS Monograph, U.S. Department of Commerce, USA. <https://doi.org/10.6028/NBS.MONO.25-18>
- [33] Tran, T.N., Pham, T.V.A., Le, M.L.P., Nguyen, T.P.T. (2013). Synthesis of amorphous silica and sulfonic acid functionalized silica used as reinforced phase for polymer electrolyte membrane. *Advances in Natural Sciences: Nanoscience and Nanotechnology*, 4(4): 045007. <http://doi.org/10.1088/2043-6262/4/4/045007>
- [34] Yadav, D., Nirala, A., Kumar, R., Singh, P.K. (2021). Density variation in nanofluids as a function of concentration and temperature. *Materials Today: Proceedings*, 46: 6576-6580. <http://doi.org/10.1016/j.matpr.2021.04.052>
- [35] Zhang, Y., Hammoodi, K.A., Sajadi, S.M., Li, Z., Jasim, D.J., Nasajpour-Esfahani, N., Salahshour, S., Eftekhari, S.A., Khabaz, M.K. (2024). Obtaining an accurate prediction model for viscosity of a new nano-lubricant containing multi-Walled carbon nanotube-Titanium dioxide nanoparticles with oil SAE50. *Tribology International*, 191: 109185. <http://doi.org/10.1016/j.triboint.2023.109185>
- [36] Huminc, G., Huminc, A. (2018). Hybrid nanofluids for heat transfer applications-A state-of-the-art review. *International Journal of Heat and Mass Transfer*, 125: 82-103. <http://doi.org/10.1016/j.ijheatmasstransfer.2018.04.059>
- [37] Kotia, A., Borkakoti, S., Deval, P., Ghosh, S.K. (2017). Review of interfacial layer's effect on thermal conductivity in nanofluid. *Heat and Mass Transfer*, 53: 2199-2209. <http://doi.org/10.1007/s00231-016-1963-6>
- [38] Bakhtiari, R., Kamkari, B., Afrand, M., Abdollahi, A. (2021). Preparation of stable TiO₂-Graphene/Water hybrid nanofluids and development of a new correlation for thermal conductivity. *Powder Technology*, 385: 466-477. <http://doi.org/10.1016/j.powtec.2021.03.010>

NOMENCLATURE

<i>A</i>	area, m ²
<i>C_p</i>	specific heat at constant pressure, J/ (kg K)
<i>k</i>	thermal conductivity, W/(m·K)
<i>m</i>	mass, kg
<i>Q</i>	heat, W
<i>R</i>	radius, m
<i>T</i>	temperature, K
<i>V</i>	volume, m ³

Greek symbols

ρ	density, kg/m ³
φ	nanofluids volume fraction

Subscripts

f	base fluid
nl	nanolubricant
p	particle